



## Methoxylation of $\alpha$ -pinene over mesoporous carbons and microporous carbons: A comparative study



Inês Matos<sup>a,d,\*</sup>, Marta F. Silva<sup>a</sup>, Ramiro Ruiz-Rosas<sup>b</sup>, Joaquim Vital<sup>a</sup>, José Rodríguez-Mirasol<sup>b</sup>, T. Cordero<sup>b</sup>, José E. Castanheiro<sup>c,\*</sup>, Isabel M. Fonseca<sup>a</sup>

<sup>a</sup> REQUIMTE, CQFB, FCT, Universidade Nova de Lisboa, 2829-516 Caparica, Portugal

<sup>b</sup> Chemical Engineering Department, School of Industrial Engineering, University of Málaga, c/Doctor Ortiz Ramos s/n, Campus de Teatinos, 29071 Málaga, Spain

<sup>c</sup> Centro de Química de Évora, DQ, Universidade de Évora, 7000-671 Évora, Portugal

<sup>d</sup> Instituto Politécnico de Setúbal, ESTBarreiro, 2839-001 Barreiro, Portugal

### ARTICLE INFO

#### Article history:

Received 11 May 2014

Received in revised form 14 July 2014

Accepted 2 August 2014

Available online 12 August 2014

#### Keywords:

Activated carbon

Pinene methoxylation

Biomass carbon

Acid catalyst

### ABSTRACT

A biomass derived carbon, a commercial microporous carbon and a xerogel mesoporous carbon catalysts were used in the study of  $\alpha$ -pinene methoxylation reaction and the influence of textural and physical-chemical properties of the carbons was evaluated. Biomass carbon presented the higher activity, whereas the commercial one is the less active in the conditions studied. The main product of the reaction was  $\alpha$ -terpinyl methyl ether and good values of selectivity were obtained over all the catalysts.

A kinetic model was developed assuming that the  $\alpha$ -pinene is consumed according to the parallel reaction network. The kinetic model presents high quality fittings to the experimental concentration profiles.

These results show that it is possible to activate a waste residue using  $H_3PO_4$  and convert it to high added value product such as acid catalyst.

© 2014 Elsevier Inc. All rights reserved.

### 1. Introduction

Biomass is already playing an important role in finding answers for some of the challenges society faces today. Along with the raise in environmental concern combined with the need for a sustainable development there is a pressing need to reduce our fossil fuel and fossil derived chemicals dependence [1]. In 2050 it is expected that a significant part of the fuels needed, will be produced from biomass, in the same way biomass should also be used as feedstock in the production of chemicals [2].

Monoterpenes are renewable resources that are widely used in the pharmaceutical, cosmetic and food industries. Among them  $\alpha$ -Pinene is a readily available and inexpensive raw material usually obtained from pine gum or as a waste from the Kraft process. Several transformations of this material, such as acetoxilation, isomerization, oxidation, among others can be applied to obtain a wide variety of added value products [3–6]. In particular the main product of the methoxylation catalyzed reaction is  $\alpha$ -terpinyl methyl ether. This compound smells grapefruit-like and finds application as flavor and fragrance for perfume and cosmetic products [7].

When strong mineral acids are used as catalysts for this transformation, the environmental and economic disadvantages are well known. One of the areas that can have a great contribution to overcome these problems is the development of catalysts leading to reactions more energetically efficient, more selective and less hazardous. The use of solids as catalytic materials in liquid-phase reactions as replacement for homogeneous catalysts has recently been a major goal in catalysis research. Easy recovery without the need of aqueous treatment during work-up procedures, and the possibility of regeneration are among the advantages of the application of heterogeneous catalysts resulting in a reduction of the environmental impact.

There has been an effort to use porous solid materials as catalysts for the  $\alpha$ -pinene alkoxylation and catalysts like Beta zeolite, mesoporous silicas, silica supported heteropolyacids have been reported [8–10]. Nevertheless more efficient and less expensive catalysts are still on demand for this and other reactions.

Activated carbon is a rather inexpensive material that presents enormous versatility and is extremely environmental friendly. Apart from high chemical and physical stability, one of the most interesting features of activated carbons is their porous structure that, depending on the precursor and preparation method, is very tuneable. These materials have found applications in different areas such as adsorption of pollutants [11,12] separation and purification [13], and also in catalysis [14–17]. Obtaining low cost

\* Corresponding authors. Address: REQUIMTE, CQFB, FCT, Universidade Nova de Lisboa, 2829-516 Caparica, Portugal.

E-mail addresses: [ines.am.matos@gmail.com](mailto:ines.am.matos@gmail.com) (I. Matos), [jefc@uevora.pt](mailto:jefc@uevora.pt) (J.E. Castanheiro).

activated carbons have attracted many researchers attention and several lignocellulosic materials have been studied as precursors [18–20]. Biomass derived carbons have been presented as a suitable pathway for the valorisation of residues. The application of these activated carbons in catalysis for green chemistry represents an extra effort towards sustainability. Activated carbon materials from biomass waste can be produced by physical or chemical activation, but one can consider some advantages in chemical activation, such as the single step process, the combination of carbonization and activation and the relatively lower temperatures [21]. Particularly chemical activation with phosphoric acid may generate phosphorous containing surface functional groups, thus conferring higher surface acidity to the carbon [17]. Furthermore the acid groups of the carbons obtained by this single step have demonstrated high-thermal stability and the obtained carbons present high-structural thermal stability [22].

This work presents the role of the textural properties of the activated carbons in the catalytic activity for  $\alpha$ -pinene methoxylation reaction. The studied carbons were chemically treated to introduce functional groups. For this purpose, microporous-mesoporous and mesoporous carbons have been used. The bi-modal pore structure activated carbon was prepared by chemical activation with  $H_3PO_4$  of olive stones, a waste from the food industry, whereas, the mesoporous carbon was synthesised by the sol gel method. A commercial activated, carbon obtained by physical activation of biomass residue (coconut shells), was also used for comparison. In order to gain further insight on this reaction a kinetic model was developed and used to described some of the results.

## 2. Experimental

### 2.1. Preparation of the catalysts

Biomass derived carbon was prepared as described earlier [22]. Olive stones were supplied by Sca Coop. And. Olivarera y Frutera San Isidro (Periana, Malaga). After grinding the olive stone, the precursors were impregnated with  $H_3PO_4$  85% (w/w) aqueous solution ( $H_3PO_4$ /precursor mass ratio = 2) at room temperature and dried for 24 h at 60 °C. The impregnated substrates were activated under continuous  $N_2$  flow (150 mL/min STP) at 600 °C. Subsequently the activated sample was washed with distilled water at 60 °C until neutral pH and negative phosphate analysis in the eluate. Carbon CB was obtained.

The mesoporous carbon sample was prepared according Lin and Ritter [23] by sol-gel technique. All reagents and solvents used in the preparation of resorcinol/formaldehyde (RF) aqueous gels and surface functionalization of the carbon xerogels were purchased from Aldrich and used as received.

An aqueous solution of resorcinol (R), formaldehyde (F) and sodium carbonate (C), was prepared in such a way that the solid material is 5% (wt./v) of the total volume, and in which the R/F mole ratio was fixed at 1:2 and the R/C mole ratio was fixed at 50:1.

The initial pH of the solution was adjusted to 6.10–6.20 with diluted  $HNO_3$ . The solution was sealed in a flask and magnetically stirred during 1 h. This procedure was followed by a thermal treatment at  $85 \pm 3$  °C during a week, without stirring. The gel obtained was washed with acetone for 3 days. Afterward it was dried under  $N_2$  atmosphere in a tube furnace using a heating rate of 0.5 °C/min. The temperature was heated up to 65 °C and then held there for 5 h, raised up to 110 °C and kept there for another 5 h. Finally, the carbon xerogel was formed by pyrolysis of the dried gel at 800 °C for 3 h in a  $N_2$  atmosphere with both heating and cooling rates set at 0.5 °C/min (CM).

A commercial carbon from Norit was used for comparison purposes. This is also a biomass based carbon, derived from coconut shells but using physical activation.

For the oxidation of the carbon surface, the carbon xerogel (CM), the  $H_3PO_4$  activated biomass carbon (CB) and the commercial Norit carbon were refluxed with a nitric acid solution (13 M) for 6 h (1 g/20 mL). After cooling the materials were washed with deionized water in soxhlet until neutral pH and then dried in oven at 110 °C, thus obtaining the catalyst CMN, CBN and NoritN, respectively.

The introduction of sulfonic groups in the carbon xerogel surface was achieved by placing the oxidized mesoporous carbon (CMN) in a concentrated sulfuric acid solution (1 g carbon/20 mL sulfuric acid solution) and heating it at 150 °C for 13 h under  $N_2$  atmosphere. The obtained catalyst was washed with deionized water in soxhlet until pH 7 and then dried in oven at 110 °C (carbon CMNS).

### 2.2. Characterization of the catalyst

Textural characterization by  $N_2$  adsorption at 77 K was performed on an ASAP 2010 V1.01 B Micromeritics. Samples were degasified at 120 °C for 24 h. The apparent specific surface area was determined using the BET method. Microporous volume and mesoporous surface area were determined by the t-method, using a standard isotherm proposed by Greg and Sing [24].

Temperature-programmed desorption analyses (TPD-MS) were carried out using a Micromeritics TPD/TPR 2900 instrument, coupled with a mass spectrometer Fisons MD800 (Leicestershire, UK) instrument for the monitoring of CO ( $m/z$  28) and CO ( $m/z$  44) evolution. Prior to analysis, the sample (ca. 50 mg) was placed in a fixed bed U-shaped quartz tubular micro-reactor and dried at 383 K in flowing He, overnight. The temperature was increased at a rate of 10 K/min to 1273 K, under a flow of helium (25 mL/min, 0.1 MPa).

Elemental analysis of the carbons was carried out in a CHNS Analyser (ThermoFinnigan Flash, EA, 1112 series). Oxygen content was obtained by the difference between the total percentage (100 wt%) and the sum of percentages (wt%) of nitrogen, carbon, hydrogen and sulfur.

The surface chemistry of the samples was analyzed by X-ray photoelectron spectroscopy (XPS) using a 5700C model Physical Electronics apparatus with  $MgK\alpha$  radiation (1253.6 eV). For the analysis of the XPS peaks, the C1s peak position was set at 284.5 eV and used as reference to locate the other peaks. The fitting of the XPS peaks was done by least squares using Gaussian-Lorentzian peak shapes. The phosphorus spectrum of biomass carbon was deconvoluted using two doublet peaks with an area ratio of 0.5 and a separation between peaks of 0.84 eV [25].

### 2.3. Catalytic experiments

The catalytic experiments were carried out in a stirred batch reactor with reflux, at different temperatures (50–65 °C) and at atmospheric pressure. In a typical experiment, the reactor was loaded with 50 mL of methanol and 0.2 g of catalyst. Reactions were started by adding the desired amount of  $\alpha$ -pinene (3–12 mmol). Particle sizes of the catalysts were maintained between 100 and 300  $\mu$ m. Stirring rate was kept in high value (1000 rpm) to minimize external mass transfer limitations.

Nonane was used as the internal standard. Samples were taken periodically and analyzed by GC, using a KONIC HRGC-3000C instrument equipped with a 30 m  $\times$  0.25 mm DB-1 column.

## 3. Results and discussion

### 3.1. Catalyst characterization

The different activated carbons were characterized after the oxidation of the surface to determine the features of the catalysts.

Some characterization data of the parent carbons before oxidation is also presented.

Samples CM, CMN and CMNS presented a nitrogen adsorption–desorption isotherms at 77 K type IV as expected for mesoporous materials. Also the original CB sample showed a type IV isotherm with a close hysteresis loop, characteristic of solids with a broad pore size distribution with meso and micropores contribution. After the  $\text{HNO}_3$  treatment, the nitrogen uptake lowered and the shape shifted to type I for sample CBN. On the other hand, samples Norit and NoritN present type I isotherms, characteristic of microporous materials. The Nitrogen adsorption–desorption isotherms of the commercial activated carbon NoritN also shows a hysteresis type H4.

The textural properties and elemental composition of the activated carbons are collected in Table 1. It should be noted that oxygen amount has been corrected to reflect the presence of phosphorus and sulfur in CB, CBN and CMNS samples. The  $\text{H}_3\text{PO}_4$  activated biomass derived carbons and the commercial carbons (CB and Norit) show the highest BET area and microporous volume. After oxidation treatment with  $\text{HNO}_3$ , NoritN presents higher difference between the microporous volume and the total pore volume meaning that the retained amount of meso and macroporous is higher for the commercial carbon than for the biomass derived carbon. CBN preserves a high microporous volume, indicating that by using the described procedure it is possible to obtain biomass-based and functionalized activated carbon with high microporosity. Nevertheless the oxidation treatment led to some structure changes in the biomass carbon. It did not only display a loss in surface area and micropore volume, which can be related to a preferential oxidation on the micropore mouths that produces blockage of part of the microporosity, but it also showed a huge decrease in the mesopore volume. A previous work revealed that mesoporosity on the CB is mainly located at the external surface of the carbon particle [22], P-containing carbons, as CB, are gasified following a shrinking core model.  $\text{N}_2$  adsorption isotherms of partially gasified samples proved that mesoporosity, which is usually located in the most external part of the carbon particles, was destroyed during the gasification of the carbon at burn-offs lower than 35%, without any macroporosity development. Thus the aggressive oxidation treatment may be eroding the particle surface, destructing the mesoporosity. In contrast the textural properties of the carbon xerogel seem not to be greatly affected by the acid treatment thus indicating that this is a more ordered and stable structure with a lower amount of sites susceptibles of being oxidized and form surface oxygen groups. Elemental analysis of the catalyst samples also revealed that the mesoporous carbon catalyst is probably the carbon material more difficult to oxidize since it is the one with the lower uptake of oxygen after treatment with Nitric acid. The commercial Norit carbon shows the higher amount of oxygen, while CBN carbon seems to develop surface nitrogen groups after the  $\text{HNO}_3$  treatment.

Further characterization of the surface chemistry was attained by TPD analysis of the samples. By this technique it is possible to

infer in the functional groups present in each sample surface. Fig. 1 presents the TPD curves for the 3 catalysts NoritN, CBN, and CMN. The deconvolution of the CO and  $\text{CO}_2$  TPD curves, following the method previously described elsewhere [26], allows the determination of the contribution of different surface groups. According to the literature [27,28] some general trends may be applied to the assignment of the deconvoluted peaks. The peaks in the  $\text{CO}_2$  curve can be assigned to carboxylic groups, carboxylic anhydride and lactones. In the CO curves there will be contribution from phenol groups, the carboxylic anhydride groups, and also from the carbonyl, quinone and ether altogether. Besides, another contribution was assigned in TPD obtained from the CB samples, being related to the thermal reduction of the surface phosphorus groups. Since the decomposition of carboxylic anhydrides will contribute to both CO and  $\text{CO}_2$  profiles, there will be a peak with the same area and half width in each profile of the same sample. The obtained results are presented in Fig. 2.

Eventhough the bulk characterization by elemental analysis indicated that the oxidized commercial carbon would have the higher amount of oxygen, TPD results show that it is the oxidized biomass derived carbon the one with more surface functional groups. This carbon seems to be more easily modified albeit with some cost to the textural properties. Moreover, it shows a very distinctive peak at temperatures ranging from 750 to 850 °C in the CO-TPD that has been assigned elsewhere to the decomposition of the C–O–P bond from the phosphonate groups [20]. The presence of these phosphonate groups endorses strong acid catalyst function to the carbon surface, which has been proven by the high activity in alcohol dehydration for similar biomass based  $\text{H}_3\text{PO}_4$ -activated carbons [17,29–31]. The nitric acid oxidation of this carbon seems to introduce a higher heterogeneity degree in these species, reflected in the widening of the related peak. It also shows a small reduction in the C–O–P amount, that must come from P groups that were placed in the mesoporosity and were released during the destruction of the external porosity after the acid treatment. In addition CBN sample has the higher amount of carboxylic acid groups in the surface which are expected to be a very active catalytic centers. It is interesting that for the commercial norit carbon the amount of carboxylic groups introduced is similar to the amount of phenol groups which are less acidic.

As mentioned before, the CB carbon was obtained from olive stones using phosphoric acid in the preparation procedure as activating agent. It has been reported in the literature [32] that it is possible that some phosphate groups are formed in the surface of the carbon. The presence of such groups may confer different properties to the catalyst as they can act as another active catalytic center [17]. Besides the different oxygen surface groups, already identified by TPD, the XPS study of sample CB confirmed the presence of phosphorous in the surface of the carbon with a XPS P2p peaks of maxima binding energy around 132.5–133.5 eV (Fig. 3). The P2p zone is the result of the contribution of three different phosphorus that can be described as P groups bonded to a carbon site with a bridge O atom ( $\text{COPO}_3$  or  $(\text{CO})_3\text{PO}$  groups, 134.2 eV),

**Table 1**  
Textural characterization and elemental analysis.

Catalyst	$S_{\text{BET}}$ ( $\text{m}^2/\text{g}$ ) BET	$V_{\text{mic}}$ ( $\text{cm}^3/\text{g}$ ) <i>t</i> method	$V_{\text{p}}$ ( $\text{cm}^3/\text{g}$ ) gurvitsch	Elemental analysis			
				C (%)	H (%)	N (%)	O (%)
Norit	926	0.35	0.61	90.25	0.38	0.38	8.99
NoritN	829	0.25	0.47	72.01	0.66	1.04	26.29
CB	1456	0.60	0.82	87.12	1.68	0.18	6.82
CBN	887	0.37	0.40	76.36	1.24	1.40	18.90
CM	665	0.17	0.36	82.53	0.80	0.15	16.52
CMN	622	0.16	0.34	78.27	1.19	0.83	19.72
CMNS	669	0.18	0.36	75.20	1.09	0.28	23.44

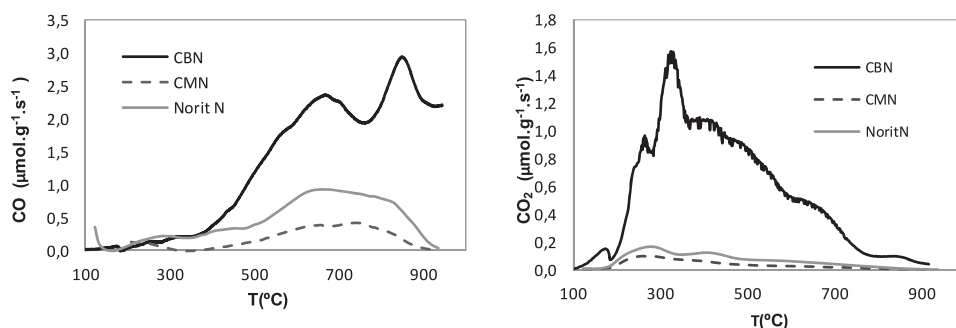


Fig. 1. TPD study of the 3 catalysts. CO and CO<sub>2</sub> TPD spectra of NoritN, CBN and CMN.

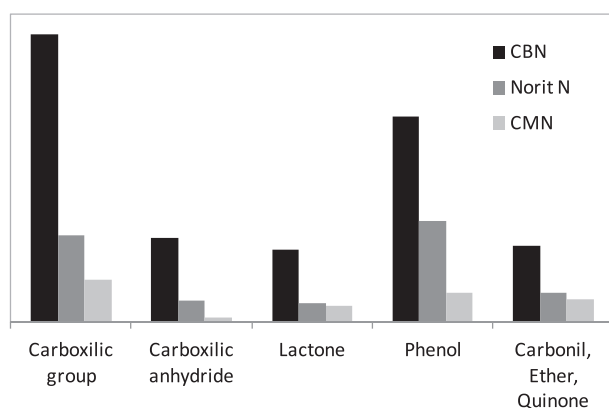


Fig. 2. TPD study: comparative amount of oxygen containing surface groups determined by integration of the TPD deconvoluted curves.

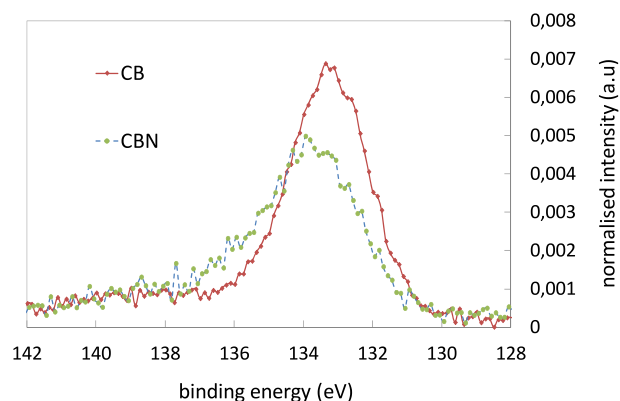


Fig. 3. XPS spectrum of the samples CB and CBN displaying the P2p peak.

directly bonded to a carbon site (CPO<sub>3</sub> or C<sub>2</sub>PO<sub>2</sub> groups, 133.2 eV), or C<sub>3</sub>PO groups (132.0 eV) [17,25,33]. The P2p spectra has been deconvoluted considering such binding energy assignments and results are enlisted in Table 2. The liquid oxidation treatment results in shift to higher binding energies of the entire signal. This result suggests that the oxidation treatment is able to oxidize not only the carbon surface but also the phosphorus groups. This is supported by the deconvolution results, where most of C<sub>3</sub>PO groups are oxidized to either CPO<sub>3</sub> or COPO<sub>3</sub> oxygenated phosphorus surface groups, which turns to be those more active for acid catalyzed reactions. Even after the treatment with nitric acid and subsequent thorough washing of the activated carbon, most of the phosphorus remains linked to the carbon surface, which points out the stability of such groups.

### 3.2. Catalytic study

The main purpose of these studies was to compare activated carbon with different textural and physicochemical properties in the methoxylation of  $\alpha$ -pinene. In this way it may be possible to determine the importance of the different catalyst characteristics for this particular reaction. Fig. 4 shows the conversion with time and the initial activity of the 3 catalysts. CBN presents the higher value, followed by CMN and NoritN.

Table 2  
Atomic % of elements and surface P group distribution by XPS.

Sample	Atomic concentration				P group distribution		
	C (%)	N (%)	O (%)	P (%)	CPO (%)	CPO <sub>3</sub> (%)	COPO <sub>3</sub> (%)
CB	88.1	0.3	10.0	1.6	26	55	20
CBN	74.6	1.5	22.5	1.4	3	54	43

The two microporous catalysts present similar surface area but the commercial catalyst has more mesoporous which can act as transport porous and facilitate the access to the active site. This feature, however, was not enough to ensure higher catalytic activity.

On the other hand the textural properties do play some role in activity, and mesoporosity may be an important factor determining it. The mesoporous xerogel carbon presents higher activity than the microporous commercial one. In this case it is possible that mesoporous xerogel carbon have their active sites more exposed, whereas the microporous carbon Norit may have part of them in pores inaccessible for the solution.

The main product of  $\alpha$ -pinene (1) methoxylation was  $\alpha$ -terpinyl methyl ether (2) but simultaneously several by products are also formed:  $\gamma$ -terpinyl methyl ether (3),  $\beta$ -terpinyl methyl ether (4), terpinolene (5), limonene (6), endo-bornyl methyl ether (7),  $\beta$ -fenchyl methyl ether (8), exobornyl methyl ether (9), bornylene (10) and camphene (11) (Scheme 1).

The alkoxylation of  $\alpha$ -pinene initiates by protonation of the  $\alpha$ -pinene double bond to form the pinyl ion (A). The reaction then proceeds via two parallel pathways depending on the pinyl ion rearrangement, one of which resulting in by-cyclic products (route A) and the other in monocyclic products (route B).

The three catalysts present similar values of selectivity at maximum conversion. Fig. 5 represents the relation of selectivity with conversion and it is observed that there are little differences between catalysts, probably because of the similar nature of the active groups. With all catalysts approximately 50% selectivity to  $\alpha$ -terpinyl methyl ether was observed.

To further access the influence of different active centers in the carbon surface a fourth catalyst was prepared and tested in similar reaction conditions. The mesoporous xerogel carbon and the biomass derived carbon after oxidation were submitted to yet another acid treatment with sulfuric acid with the purpose of introducing

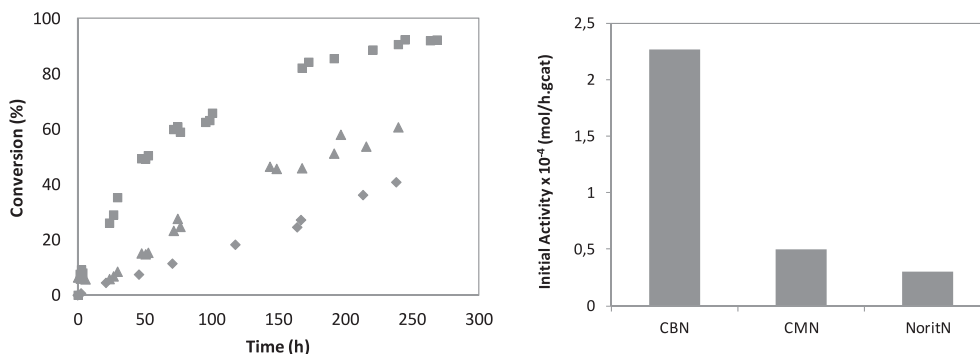
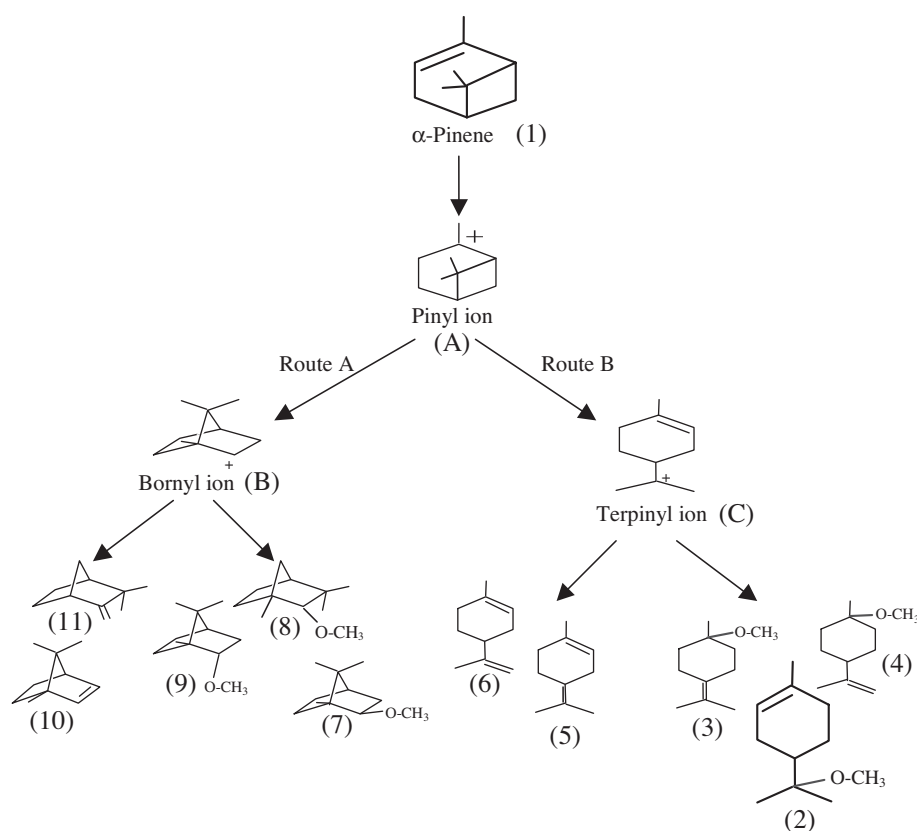


**Fig. 4.** Methoxylation of  $\alpha$ -pinene over activated carbon catalysts. (a) Conversion vs. time. (b) Initial activity of the 3 catalysts. Initial activities taken as the maximum observed reaction rate, calculated from the maximum slope of the  $\alpha$ -pinene kinetic curve. Reaction conditions:  $T = 60^\circ\text{C}$ ;  $m_{\text{cat}} = 0,2 \text{ g}$ ;  $n_{\alpha\text{-pinene}} = 9 \text{ mmol}$ ; 50 ml of methanol. (■) CBN; (▲) CMN; (◆) NoritN.



**Scheme 1.** Mechanism of alfa-pinene methoxylation.

sulfonic groups in the surface. These functional groups are expected to be stronger active centers in acid catalyzed reactions. For the biomass derived carbon these procedure prove to be overly aggressive and most of the textural properties were lost (results not showed). In the case of the xerogel carbon, the TPD study of the obtained catalyst (CMNS) confirmed the presence of sulfonic groups although in very little amount. In a previous study XPS of this sample showed also the presence of sulfonic groups [14]. The initial catalytic activity of this catalyst was 3, 5 times higher than the simply oxidized one, and the overall conversion was similar to the obtained with biomass catalyst CBN. This behavior may be due to not only the strength of the acid sites but also it is possible that these sites are more accessible. Selectivity was not greatly affected but it is a little higher with this catalyst, close to 60%. Taking all these results in consideration it seems that, even

though the nature of the active sites may have an important role, it is probably the amount of active sites what is determining the overall activity.

The effect of several parameters in the reaction was evaluated to determine the optimized reaction conditions. This study was focused on the biomass carbon for it is the most promising catalyst. Lowering the reaction temperature resulted in big loss in activity. The exponential dependence on temperature confirms that the reaction system is working on the kinetic control regime and so the reaction temperature was kept at  $60^\circ\text{C}$  for the completion of the study.

The initial concentration of  $\alpha$ -pinene was varied from 0.06 M to 0.23 M, whilst the temperature ( $60^\circ\text{C}$ ) and the catalyst loading were kept constant (0.2 g). The conversion concentration profiles were not greatly changed. This may be an indication that

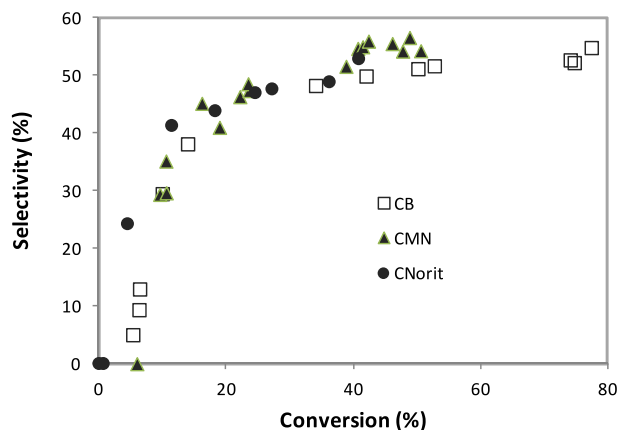


**Fig. 5.** Methoxylation of  $\alpha$ -pinene. Selectivity to  $\alpha$ -terpinyl methyl ether: (□) CBN; (▲) CMN; (●) NoritN. Reaction conditions:  $T = 60^\circ\text{C}$ ;  $m_{\text{cat}} = 0.2\text{ g}$ ;  $n_{\alpha\text{-pinene}} = 9\text{ mmol}$ ; 50 ml of methanol.

adsorption of  $\alpha$ -pinene with the formation of a monolayer is taking place, thus the same amount of  $\alpha$ -pinene is accessible to the active site no matter what the initial concentration is.

The variation of the catalyst loading is represented in Fig. 6. This study revealed that increasing the amount of catalyst, the conversion increases with time which is probably related with the corresponding increase in active centers. However, increasing the amount of catalyst from 0.2 g to 0.4 g produces just a small increment in conversion thus indicating there is no advantage in using higher amounts. Selectivity is not affected by the changes in catalyst loading (about 60% at the highest conversion).

An important feature of heterogeneous catalyst is the possibility of reutilization. In order to study the catalyst stability a second consecutive run was carried out. A sharp decrease in activity was observed in the second utilization. Selectivity, though, was not affected. Some of the functional groups in the carbon surface seem to have been modified by a secondary reaction; it is probable that the esterification of the acid groups is occurring due to the excess of methanol present in the reaction medium. On the other hand the catalytic activity presented by the catalyst upon second utilization is only slightly higher than the presented by the pristine CB (25 vs. 22% after 250 h), this may mean that the phosphorous containing groups are more stable than the carboxylic groups formed by surface oxidation. This seems to be confirmed by the P2p spectra of CB and CBN catalyst after being used in reaction, Fig. 7. It can be seen that the oxidation state and amount of P groups is unaffected after being submitted to reaction for CB catalyst, whereas P spectra of

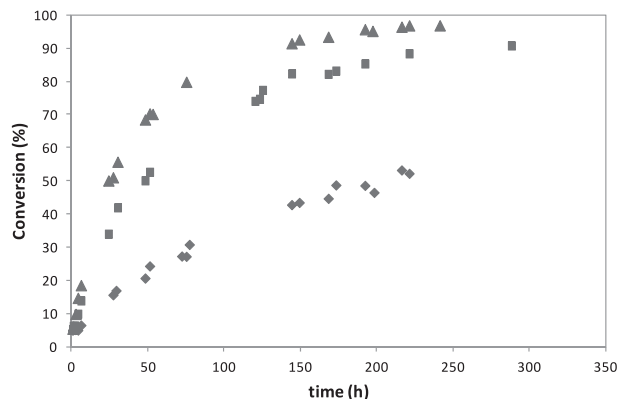


**Fig. 6.** Methoxylation of  $\alpha$ -pinene over biomass activated carbon CBN. Effect of catalyst loading. (▲) 0.4 g; (■) 0.2 g; (◆) 0.1 g. Reaction conditions:  $T = 60^\circ\text{C}$ ;  $n_{\alpha\text{-pinene}} = 9\text{ mmol}$ ; 50 ml of methanol.

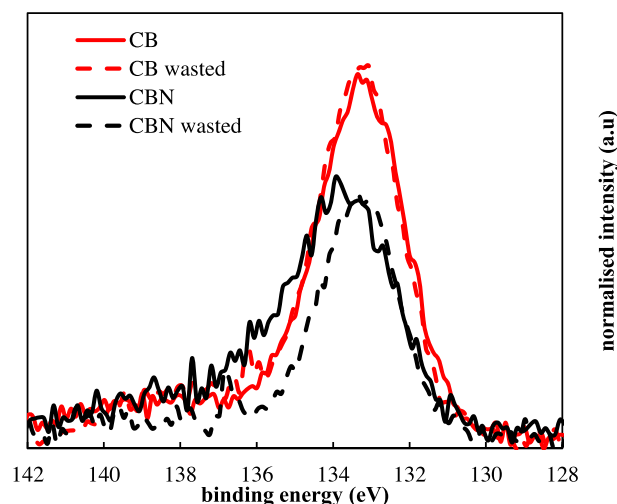


**Fig. 7.** P2p XPS photoemission region of biomass-based carbons CB and CBN before (solid line) and after being used in reaction (dashed line).

CBN, which was shifted to higher binding energies after  $\text{HNO}_3$  treatment, reverted to its original oxidation state after reaction. This can be understood as the strongly oxidized and acid  $\text{COPO}_3$  groups being deactivated after reaction, while the less oxidized  $\text{CPO}_3$  remains intact can act again as the active center for  $\alpha$ -pinene methoxylation in the second reaction test.

### 3.3. Kinetic study

A kinetic model can be a powerful instrument to better understand the mechanism involved in a catalytic reaction. A kinetic model was established considering that  $\alpha$ -pinene is consumed according to the parallel reaction network shown in Scheme 2, where P represents  $\alpha$ -pinene, E represents  $\alpha$ -terpinyl methyl ether, ME represents all the monocycle ethers formed, BE represents all the bicycle ethers formed, MH represents all monocycle hydrocarbons formed and BH represents all the bicycle hydrocarbons formed. Also the following assumptions are made:

- (1) Isothermal and isobaric reaction conditions.
- (2) As in the present case  $\alpha$ -terpinyl methyl ether seems not to be consumed, is not necessary a more complex reaction network.
- (3) Mass transfer problems are considered to be negligible
- (4) A Langmuir–Hinshelwood kinetics is assumed considering only the adsorption of the reactant  $\alpha$ -pinene.

The reaction rates of the pseudo elementary reaction are expressed as:

$$r_1 = \frac{k_1 K_p C_p}{1 + K_p \cdot C_p} \quad (1)$$

$$r_2 = \frac{k_2 K_p C_p}{1 + K_p \cdot C_p} \quad (2)$$

$$r_3 = \frac{k_3 K_p C_p}{1 + K_p \cdot C_p} \quad (3)$$

$$r_4 = \frac{k_4 K_p C_p}{1 + K_p \cdot C_p} \quad (4)$$

$$r_5 = \frac{k_5 K_p C_p}{1 + K_p \cdot C_p} \quad (5)$$

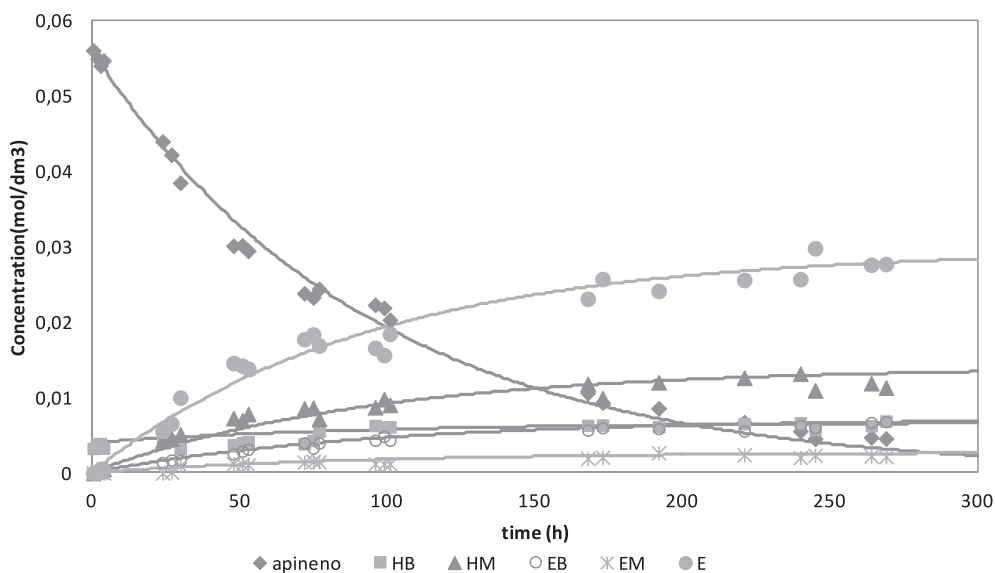
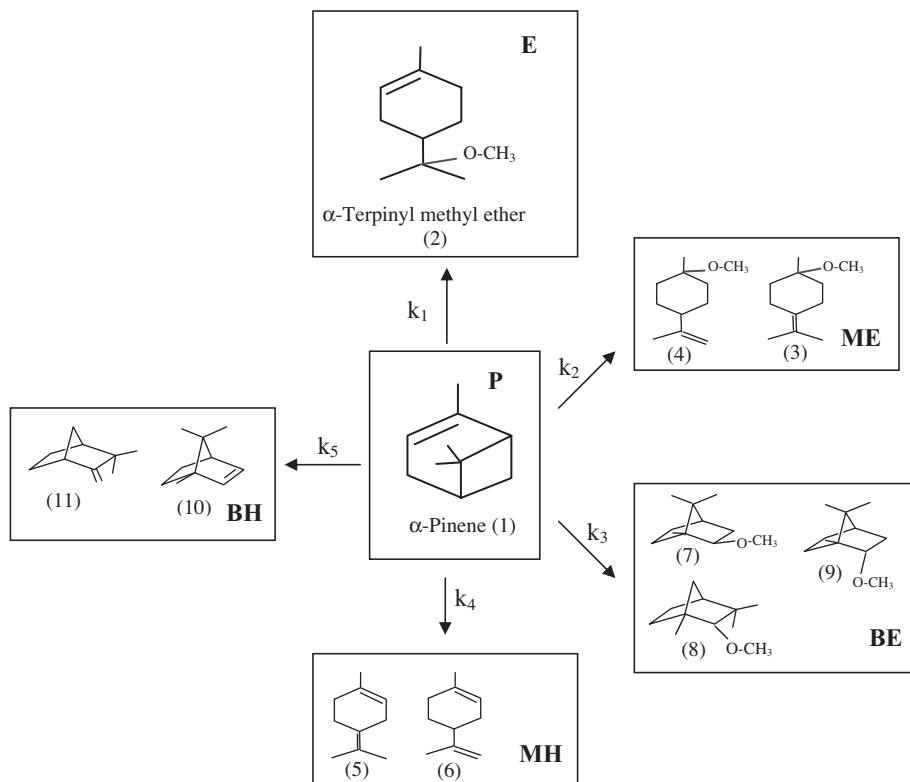


**Fig. 8.** Kinetic model fitting for catalyst CBN. The symbols are experimental data, and the lines correspond to the kinetic model.

The mole balance equations for batch reactor may be written as:

$$\frac{dC_P}{dt} = -\frac{W}{V}(r_1 + r_2 + r_3 + r_4 + r_5) \quad (6)$$

$$\frac{dC_E}{dt} = \frac{W}{V}r_1 \quad (7)$$

$$\frac{dC_{ME}}{dt} = \frac{W}{V}r_2 \quad (8)$$

$$\frac{dC_{BE}}{dt} = \frac{W}{V}r_3 \quad (9)$$

$$\frac{dC_{MH}}{dt} = \frac{W}{V}r_4 \quad (10)$$

$$\frac{dC_{BH}}{dt} = \frac{W}{V}r_5 \quad (11)$$

The optimization was carried out by the SOLVER routine in a Microsoft Excel spreadsheet.

**Table 3**

Kinetic rate constants estimated by the fitting of the model to the experimental data.

Catalyst	$k_1$ (mol/h g <sub>cat</sub> )	$k_2$ (mol/h g <sub>cat</sub> )	$k_3$ (mol/h g <sub>cat</sub> )	$k_4$ (mol/h g <sub>cat</sub> )	$k_5$ (mol/h g <sub>cat</sub> )	$K_p$ (dm <sup>3</sup> /mol)
CBN	$3.14 \times 10^{-2}$	$2.89 \times 10^{-3}$	$7.57 \times 10^{-3}$	$1.49 \times 10^{-2}$	$2.84 \times 10^{-3}$	$4.47 \times 10^{-2}$
CMN	$1.61 \times 10^{-2}$	$2.52 \times 10^{-4}$	$3.77 \times 10^{-3}$	$8.49 \times 10^{-3}$	$1.02 \times 10^{-7}$	$2.83 \times 10^{-2}$
NoritN	$2.83 \times 10^{-2}$	$2.01 \times 10^{-4}$	$9.02 \times 10^{-7}$	$6.74 \times 10^{-3}$	$7.33 \times 10^{-7}$	$2.49 \times 10^{-2}$

Since some evidence of an adsorption step was present in the experimental results a Langmuir–Hinshelwood kinetics was assumed and the fitting of the model to data points is shown in Fig. 8. The Thiele modulus and the effectiveness factor were calculated for the most active catalyst (CBN) in order to check the validity of the assumption of absence of mass transfer limitations. The mean particle radius was  $90 \pm 23 \mu\text{m}$ , and the effective diffusion coefficient of  $\alpha$ -pinene was considered to be  $2 \times 10^{-9} \text{ m}^2/\text{s}$ . The calculated Thiele modulus was 0.13, which resulted in an effectiveness coefficient higher than 95%. Therefore, internal mass diffusion effects can be considered negligible in the experimental conditions studied in this work.

It was observed that kinetic model fits experimental concentration data quite well. Table 3 shows the kinetics rate constants obtained by fitting the model to the experimental data.

Another model assuming the adsorption of the products was also tested following also a Langmuir–Hinshelwood kinetics. The results showed that the improvement in the fitting was not significant and so increasing the number of parameters was not justified.

It was observed that the CBN catalyst showed the highest activity, showing the highest values for the different kinetic rate constants. For the less active catalysts the secondary reactions seem to be less pronounced and the kinetic rate constants are one or more orders of magnitude smaller compared with the values obtained for sample CBN.

#### 4. Conclusion

Three HNO<sub>3</sub> oxidized carbon materials, a meso-microporous activated carbon prepared with biomass waste (olive stones), a xerogel carbon and a commercial microporous carbon, were successfully used as acid catalysts in the methoxylation of  $\alpha$ -pinene yielding  $\alpha$ -terpinyl methyl ether as main product of the reaction.

There are many biomass based activated carbons and different procedures to obtain them. In this paper it was used a commercial activated carbon (Norit) and an olive stone base activated carbon, both derived from biomass. The olive stone based carbon was obtained by chemical activation with phosphoric acid. It was observed that this resulted in a biomass catalyst with better characteristics for the reaction studied, resulting in a clear added value to the material. The catalytic activity increased in the order Cnorit < CMN < CB. The commercial catalyst was found to be the less suitable one.

The results also seem to indicate that the most important feature of these catalysts is the surface chemistry although some effect of the textural properties could be observed. All catalyst showed good selectivity towards the  $\alpha$ -terpinyl methyl ether. A kinetic model has been developed that accurately describes the experimental data, allowing to assess the formation of the pynil ion as the rate determining step in this reaction.

#### Acknowledgments

I. Matos thanks Fundação para Ciência e Tecnologia for Grant SFRH/BPD/34659/2007.

This work has been supported by Fundação para a Ciência e a Tecnologia- Portugal through Grant No. PEst-C/EQB/LA0006/2011 and by Ministerio de Economía y Competitividad- Spain (CTQ

2012-36408). This work was carried out also with support from the Project PTDC/CTM-POL/114579/2009.

#### Appendix A. Supplementary data

Supplementary data associated with this article can be found, in the online version, at <http://dx.doi.org/10.1016/j.micromeso.2014.08.006>.

#### References

- [1] European commission, GREEN PAPER: From Challenges to Opportunities: Towards a Common Strategic Framework for EU Research and Innovation funding, <[http://ec.europa.eu/research/csrf/pdf/com\\_2011\\_0048\\_csf\\_green\\_paper\\_en.pdf](http://ec.europa.eu/research/csrf/pdf/com_2011_0048_csf_green_paper_en.pdf)> (last accessed 24.03.2014).
- [2] M. Neelis, M. Patel, K. Blok, W. Haije, P. Bach, *Energy* 32 (2007) 1104–1123.
- [3] A. Corma, S. Iborra, A. Velty, *Chem. Rev.* 107 (2007) 2411–2502.
- [4] P. Maki-Arvela, B. Holmbom, T. Salmi, D.Y. Murzin, *Catal. Rev.* 49 (2007) 197–340.
- [5] J.E. Castanheiro, I.M. Fonseca, A.M. Ramos, R. Oliveira, J. Vital, *Catal. Today* 104 (2005) 296–304.
- [6] M.C. Ávila, N.A. Comelli, E. Rodríguez-Castellón, A. Jiménez-López, R. Carrizo Flores, E.N. Ponzi, M.I. Ponzi, *J. Mol. Catal. A* 322 (2010) 106–112.
- [7] M.R. Kare, *J. Agric. Food Chem.* 17 (1969) 677–680.
- [8] K. Hensen, C. Mahaim, W.F. Hölderich, *Appl. Catal. A* 149 (1997) 311–329.
- [9] J.E. Castanheiro, L. Guerreiro, I.M. Fonseca, A.M. Ramos, J. Vital, *Stud. Surf. Sci. Catal.* 174 (2008) 1319–1322.
- [10] D.S. Pito, I. Matos, I.M. Fonseca, A.M. Ramos, J. Vital, J.E. Castanheiro, *Appl. Catal. A* 373 (2010) 140–146.
- [11] K.Y. Foo, B.H. Hameed, *J. Hazard. Mater.* 171 (2009) 54–60.
- [12] A. Bhatnagar, W. Hogland, M. Marques, M. Sillanpää, *Chem. Eng. J.* 219 (2013) 499–511.
- [13] M.S. Shafeeyan, W.M.A.W. Daud, A. Houshmand, A. Shamiri, *J. Anal. Appl. Pyrol.* 89 (2010) 143–151.
- [14] I. Matos, P.D. Neves, J.E. Castanheiro, E. Perez-Mayoral, R. Martin-Aranda, C. Duran-Valled, J. Vital, A.M. Botelho do Rego, I.M. Fonseca, *Appl. Catal. A* 439–440 (2012) 24–30.
- [15] P. Ferreira, I.M. Fonseca, A.M. Ramos, J. Vital, J.E. Castanheiro, *Catal. Commun.* 12 (2011) 573–576.
- [16] C.J. Durán-Valle, M. Madrigal-Martínez, M. Martínez-Gallego, I.M. Fonseca, I. Matos, A.M. Botelhodorego, *Catal. Today* 187 (2012) 108–114.
- [17] J. Bedia, R. Ruiz-Rosas, J. Rodríguez-Mirasol, T. Cordero, *AIChE J.* 56 (6) (2010) 1557–1568.
- [18] A.S. Mestre, A.S. Bexiga, M. Proença, M. Andrade, M.L. Pinto, I. Matos, I.M. Fonseca, A.P. Carvalho, *Bioresour. Technol.* 102 (2011) 8253–8260.
- [19] A.S. Mestre, J. Pires, J.M.F. Nogueira, J.B. Parra, A.P. Carvalho, C.O. Ania, *Bioresour. Technol.* 100 (2009) 1720–1726.
- [20] J.M. Rosas, J. Bedia, J. Rodríguez-Mirasol, T. Cordero, *Fuel Process. Technol.* 91 (10) (2010) 1345–1354.
- [21] O. Ioannidou, A. Zabaniotou, *Renew. Sustain. Energy Rev.* 11 (9) (2007) 1966–2005.
- [22] J.M. Rosas, R. Ruiz-Rosas, J. Rodríguez-Mirasol, T. Cordero, *Carbon* 50 (2012) 1523–1537.
- [23] C. Lin, J.A. Ritter, *Carbon* 35 (1997) 1271–1278.
- [24] S.J. Gregg, K.S.W. Sing, *Adsorption, Surface Area and Porosity*, Academic Press, London, 1982.
- [25] J.F. Moulder, W.F. Stickle, P.E. Sobol, K.D. Bomben, in: J. Chastain, R.C. King Jr (Eds.), *Handbook of X-ray photoelectron spectroscopy*, Physical Electronics Inc., Eden Prairie, MN, 1995, pp. 4872–4875.
- [26] A. Valente, C. Palma, I.M. Fonseca, A.M. Ramos, J. Vital, *Carbon* 41 (2003) 2793–2803.
- [27] J.L. Figueiredo, M.F.R. Pereira, M.M.A. Freitas, J.J.M. Orfão, *Carbon* 37 (1999) 1379–1389.
- [28] N. Mahata, M.F.R. Pereira, F. Suarez-García, A. Martínez-Alonso, J.M.D. Tascon, J.L. Figueiredo, *J. Colloid Interface Sci.* 324 (2008) 150–155.
- [29] J. Bedia, R. Barrionuevo, J. Rodríguez-Mirasol, T. Cordero, *Appl. Catal. B* 103 (2011) 302–310.
- [30] J. Bedia, J.M. Rosas, D. Vera, J. Rodríguez-Mirasol, T. Cordero, *Catal. Today* 158 (2010) 89–96.
- [31] J. Bedia, J.M. Rosas, J. Rodríguez-Mirasol, T. Cordero, *J. Catal.* 271 (2010) 33–42.
- [32] J.M. Rosas, J. Bedia, J. Rodríguez-Mirasol, T. Cordero, *Fuel* 88 (2009) 19–26.
- [33] X. Wu, L.R. Radovic, *Carbon* 44 (2006) 141–151.